iScience

CellPress

Article

ALDH1A3 Regulations of Matricellular Proteins Promote Vascular Smooth Muscle Cell Proliferation

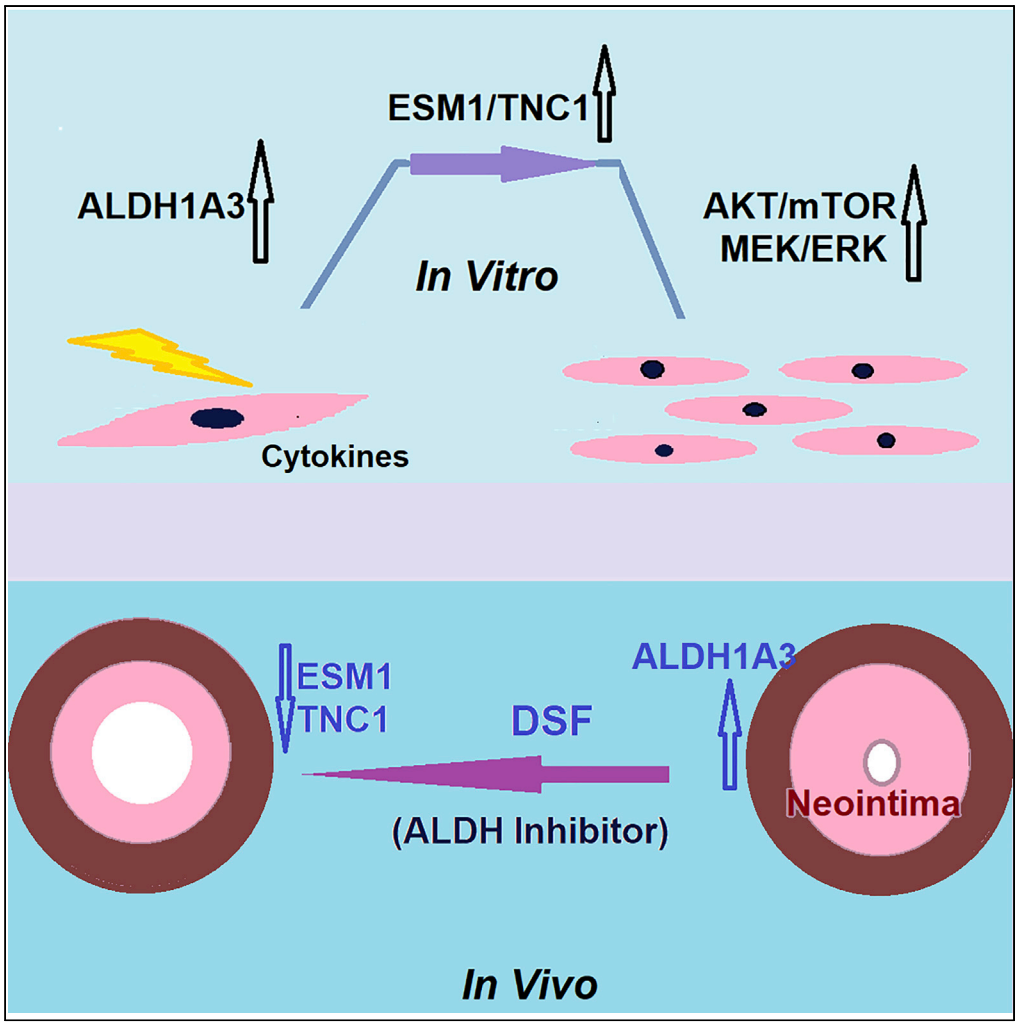

Xiujie Xie, Go Urabe, Lynn Marcho, Matthew Stratton, Lian-Wang Guo, Craig K. Kent

lianwang.guo@osumc.edu (L.-W.G.)
kc.kent@osumc.edu (C.K.K.)

HIGHLIGHTS

The ALDH1A3 isoform promotes vascular smooth muscle cell proliferation

ALDH1A3's function is mediated by its upregulation of TNC1 and ESM1

The pan-ALDH inhibitor drug disulfiram mitigates intimal hyperplasia

Xie et al., iScience *19*, 872–882
September 27, 2019 © 2019 The Authors.
https://doi.org/10.1016/j.isci.2019.08.044

iScience

CellPress

Article

ALDH1A3 Regulations of Matricellular Proteins Promote Vascular Smooth Muscle Cell Proliferation

Xiujie Xie,[1] Go Urabe,[1,2] Lynn Marcho,[1,2] Matthew Stratton,[2] Lian-Wang Guo,[1,2,3,*] and Craig K. Kent[1,*]

SUMMARY

Vascular smooth muscle cell (VSMC) proliferation promotes intimal hyperplasia (IH) in occluding vascular diseases. Here we identified a positive role of ALDH1A3 (an aldehyde dehydrogenase) in this pro-IH process. The expression of ALDH1A3, but not that of 18 other isoforms of the ALDH family, was substantially increased in cytokine-stimulated VSMCs. PDGF(BB) stimulated VSMC total ALDH activity and proliferation, whereas ALDH1A3 silencing abolished this effect. ALDH1A3 silencing also diminished the expression of two matricellular proteins (TNC1 and ESM1), revealing a previously unrecognized ALDH1A3 function. Loss-of-function experiments demonstrated that TNC1 and ESM1 mediated ALDH1A3's pro-proliferative function via activation of AKT/mTOR and/or MEK/ERK pathways. Furthermore, ALDH inhibition with disulfiram blocked VSMC proliferation/migration *in vitro* and decreased TNC1 and ESM1 and IH in angioplasty-injured rat carotid arteries. Thus, ALDH1A3 promotes VSMC proliferation at least partially through TNC1/ESM1 upregulation; dampening excessive ALDH1A3 activity represents a potential approach to IH mitigation.

INTRODUCTION

Over one million vascular reconstructions are performed in the United States each year, including coronary artery angioplasty/stenting or bypass vein grafting, arteriovenous fistula for dialysis access, and allograft transplantation. Unfortunately, (*neo*)intimal hyperplasia (IH), which narrows the vascular lumen, can lead to short-term or long-term failure in all these treatments. It is well documented that IH is principally caused by a vascular smooth muscle cell (VSMC) transition from normal to proliferative/migratory and synthetic phenotypes (Alexander and Owens, 2012). Therefore, blocking this VSMC phenotypic transition is key to IH attenuation. There are clinically used IH-attenuating drugs, i.e., rapamycin and paclitaxel, both anti-proliferative agents. However, the efficacy of rapamycin is reduced under diabetic conditions (Woods, 2013). Moreover, both rapamycin and paclitaxel have been found to increase the incidence of endothelial dysfunction and thrombosis (Inoue et al., 2011). These limitations strongly urge research efforts for better understanding of IH biology and identification of unstudied molecular mechanisms for optimal intervention.

Traditionally deemed as merely participating in cellular metabolism, in the past decade metabolic enzymes have refreshed researchers' interest for their diverse roles. For example, metabolic reprogramming has profound effects on epigenetic mechanisms that modify chromatin and alter gene expression. Aldehyde dehydrogenases (ALDHs) are a family of enzymes consisting of 19 isoforms that have distinct and overlapping functions and substrate specificities (Marchitti et al., 2007). Recent evidence suggests a vascular protective role of ALDH2, an isoform primarily mitochondrial-localized (Daiber et al., 2009; Mali et al., 2016a, 2016b). However, whether or how the 19 ALDH isoforms differentially regulate VSMC pathobiology is poorly understood. ALDH1A3 has received recent attention as a marker of normal and cancer progenitors. It is found to play an important role in maintaining cell cycle and promoting proliferation in various cell types (Dey et al., 2015; Cui et al., 2015; Zhang et al., 2014; Hegab et al., 2014; Szabo et al., 2013; Zou et al., 2012). Whether this enzyme regulates the expression of extracellular matrix (ECM) proteins was not known.

Matricellular proteins belong to a distinct category of ECM proteins. Rather than serving as ECM structural elements, they can evoke intracellular signaling and cell state changes. As such, they typically act as mediators or modulators of environment-cell interactions (Imanaka-Yoshida, 2016). It is well known that elevated ECM production is an acquired phenotype of VSMCs that undergo pro-IH phenotypic changes when stimulated in a cytokine-rich environment (Imanaka-Yoshida, 2016; Young et al., 2015). Interestingly, recent

[1]Department of Surgery, College of Medicine, Davis Heart and Lung Research Institute, Wexner Medical Center, The Ohio State University, Columbus, OH 43210, USA

[2]Department of Physiology & Cell Biology, College of Medicine, Davis Heart and Lung Research Institute, Wexner Medical Center, The Ohio State University, Columbus, OH 43210, USA

[3]Lead Contact

*Correspondence: lianwang.guo@osumc.edu (L.-W.G.), kc.kent@osumc.edu (C.K.K.)

https://doi.org/10.1016/j.isci.2019.08.044

 © 2019 The Authors.
This is an open access article under the CC BY-NC-ND license (http://creativecommons.org/licenses/by-nc-nd/4.0/).

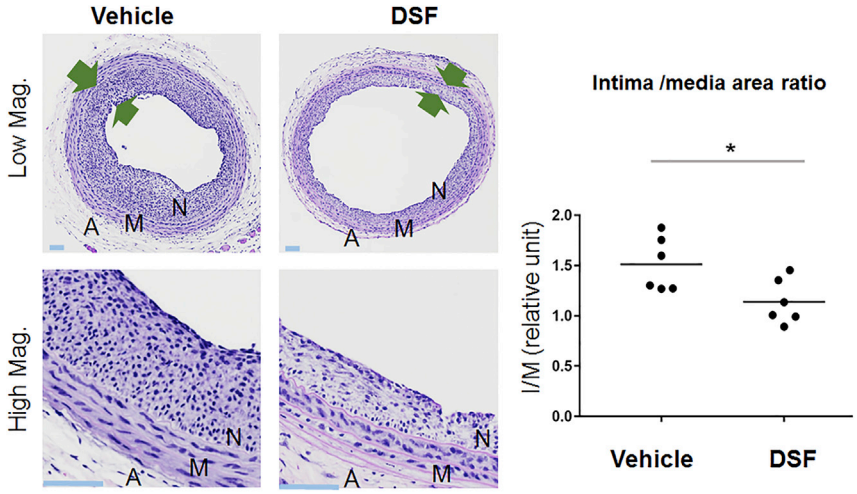

Figure 1. Perivascular Administration of DSF Reduces IH *In Vivo* in a Rat Angioplasty Model

Rat carotid artery balloon angioplasty was performed followed by periadventitial administration of disulfiram (DSF, 9 mg/rat) or vehicle control (equal amount of DMSO). The animals were euthanized 14 days later, and the arteries were collected for histological analyses.

Shown are representative H&E-stained carotid artery cross sections and quantification of the intima versus media area ratio (I/M, measure of IH). The data were generated by averaging six to eight sections from each animal. The averages from six animals in each treatment group were then averaged (see the scatterplot). *$p < 0.05$, $n = 6$ animals, Student's t test. A pair of arrows define the neointima thickness. A, adventitia; M, media; N, neointima. Scale bar: 100 μm.

literature indicates that ECM proteins, in particular matricellular proteins, reciprocally influence VSMC phenotypes via various signaling pathways (Imanaka-Yoshida, 2016; Tratwal et al., 2015). TNC1 is a typical matricellular protein implicated as important in VSMC and IH pathobiology (Ishigaki et al., 2011). A relatively less known matricellular protein, ESM1 (or endocan), was recently deemed a marker of activated endothelial cells and reported to promote IH (Balta et al., 2015). As the majority of studies on ESM1 have been focused on endothelial cells, its expression and functional regulation in VSMCs are little known. More broadly, the relationships of TNC1 and ESM1 with ALDH1A3 have not been previously explored.

We hypothesized that ALDH activity plays an important role in VSMC proliferation. Indeed, our data revealed that cytokine-stimulated ALDH activation was accompanied by VSMC proliferation, and the ALDH1A3 isoform almost entirely accounted for these changes. More significantly, we found that knocking down ALDH1A3 reduced mRNA and protein levels of TNC1 and ESM1, both pro-proliferative matricellular proteins, as indicated by our data from VSMCs. ALDH1A3 regulation of ECM proteins was unanticipated as it has not been previously reported in any cell type. Importantly, pretreatment with a clinically approved pan-ALDH inhibitor, disulfiram (DSF), reduced VSMC proliferation and migration *in vitro* and IH in a rat carotid artery balloon angioplasty model. This suggests that targeting elevated ALDH activity may provide an amenable option to mitigate IH.

RESULTS

Perivascular Administration of Disulfiram Reduces IH in a Rat Angioplasty Model

DSF is a pan-ALDH inhibitor. It was initially used to treat alcoholism and inadvertently found to have anticancer effects (Triscott et al., 2015). Considering that many alcoholic patients and/or patients with cancer may simultaneously have cardiovascular disorders, it is important to gain knowledge as to how DSF influences these disease conditions. Atherosclerosis and recurrent diseases (e.g., restenosis) following its treatment comprise the majority of vascular diseases, and they share a common etiology, i.e., IH or proliferation of the neointima. We therefore tested the effect of DSF in a well-established model of IH induced by balloon angioplasty in rat carotid arteries (Clowes et al., 1994) via perivascular administration (Wang et al., 2015) (for all methods, please refer to Supplemental Information). Animals were sacrificed at 14 days post angioplasty, and carotid arteries were collected and used for H&E staining. IH was measured as the neointima versus media area ratio. As shown in Figure 1, DSF-treated arteries displayed markedly

reduced IH than that of vehicle control. This IH-mitigating effect of DSF inspired us to further investigate the underlying molecular and cellular mechanisms.

Cytokine Stimulation Elevates ALDH Activity of VSMCs, which Is Mainly Accounted for by the ALDH1A3 Isoform

IH occurs primarily because VSMCs transition into a proliferative state (Alexander and Owens, 2012). ALDH activity has been linked to cell proliferation in cancer cells (Wang et al., 2015). We therefore explored a possible relationship between VSMC proliferation and ALDH activity. Cells were subjected to cytokine stimulation (PDGF-BB, IL-1β, TNFα, or TGFβ1) for 20 h and collected for ALDH activity assay via flow cytometry (Figure S1). The same experiment was repeated by using both human primary aortic smooth muscle cells (AoSMC) and a mouse smooth muscle cell line (MOVAS). As shown in Figures 2A and 2B, compared with solvent control, where the ALDH-active population was 5.55% and 0.91% in AoSMC and MOVAS, respectively, all cytokine treatments significantly increased ALDH-active cell populations.

We then performed assays to distinguish which isoform mainly accounted for the increased ALDH activity after cytokine stimulation. Interestingly, real-time qPCR assay indicated that, among all the 19 isoforms, only the mRNA of ALDH1A3 was significantly increased (~1.5–3 fold) in AoSMCs by stimulation with either of the four cytokines (PDGF-BB, IL1β, TNFα, or TGFβ1) (Figure 2C). In contrast, the other isoforms showed minor or insignificant changes. Cytokine-stimulated upregulation of ALDH1A3 was confirmed at the protein level by western blot assay (Figure 2D).

ALDH1A3 Genetic Silencing Abolishes PDGF-Stimulated Increase of VSMC ALDH Activity and Proliferation

We next investigated the specific role of ALDH1A3 in VSMC proliferation. Hereafter we used PDGF-BB as a stimulant throughout the *in vitro* assays. We decided to use PDGF-BB for the following considerations: (1) PDGF-BB is a mitogen that most potently stimulates VSMC proliferation and is most widely used for this experimental purpose (Wang et al., 2015). (2) Although IL1β resulted in greater stimulation of total ALDH activity than PDGF-BB (Figures 2A and 2B), ALDH1A3 protein levels stimulated by these two cytokines were essentially equal (Figure 2D). As shown in Figure 3A, western blots verified high ALDH1A3 gene knockdown efficiency. Consistent with the results presented earlier (Figure 2), PDGF-BB treatment of AoSMCs elevated ALDH activity by ~2.5 fold, whereas ALDH1A3 gene silencing abrogated this effect (Figure 3B). Furthermore, PDGF-BB stimulated AoSMC proliferation by more than 2-fold, whereas ALDH1A3 silencing nearly abolished this phenotype (Figure 3C).

Combined, these results demonstrate that ALDH1A3 is the isoform that is principally responsible for the cytokine-stimulated increase of ALDH activity that drives the VSMC phenotype change.

ALDH1A3 Genetic Silencing Diminishes the Expression of ESM1 and TNC1

We then asked the question as to what are the downstream effectors mediating ALDH1A3's regulations that lead to VSMC proliferation. We performed microarray analysis (Figure S3) to identify the genes whose expression can be upregulated by PDGF-BB in an ALDH activity-sensitive manner. By comparing the top 20 PDGF-upregulated genes with the top 20 genes whose PDGF-stimulated expression was reduced by pan-ALDH inhibition (Figure S3), we found two genes, ESM1 and TNC1, that appeared in both top-20 gene lists. To validate these two candidate genes, we determined whether ALDH1A3 knockdown changes their mRNA and protein levels. As shown by the RT-qPCR data in Figure 3D, ALDH1A3 silencing with small interfering RNA (siRNA) nearly eliminated ESM1 and TNC1 mRNAs. Moreover, the western blot data indicate that ALDH1A3 protein knockdown substantially reduced TNC1 and ESM1 proteins as well. These data revealed that ALDH1A3 potently regulates the expression of two matricellular proteins, TNC1 and ESM1.

Although TNC1 production has been previously reported to affect VSMC phenotypes (Fischer, 2007), no such report exists in the literature regarding ESM1's function. Data in Figures 3E and 3F confirm that siRNAs targeting ESM1 or TNC1 were effective in reducing target protein expression. As expected, TNC1-specific silencing largely abolished PDGF-stimulated AoSMC proliferation, consistent with the reported TNC1 function (Ishigaki et al., 2011). However, ESM1-specific silencing also effectively blocked this VSMC phenotype change, which has not been previously reported. These results suggest that TNC1 and ESM1 both are regulated by ALDH1A3 and may mediate ALDH1A3's functional effect on VSMC proliferation.

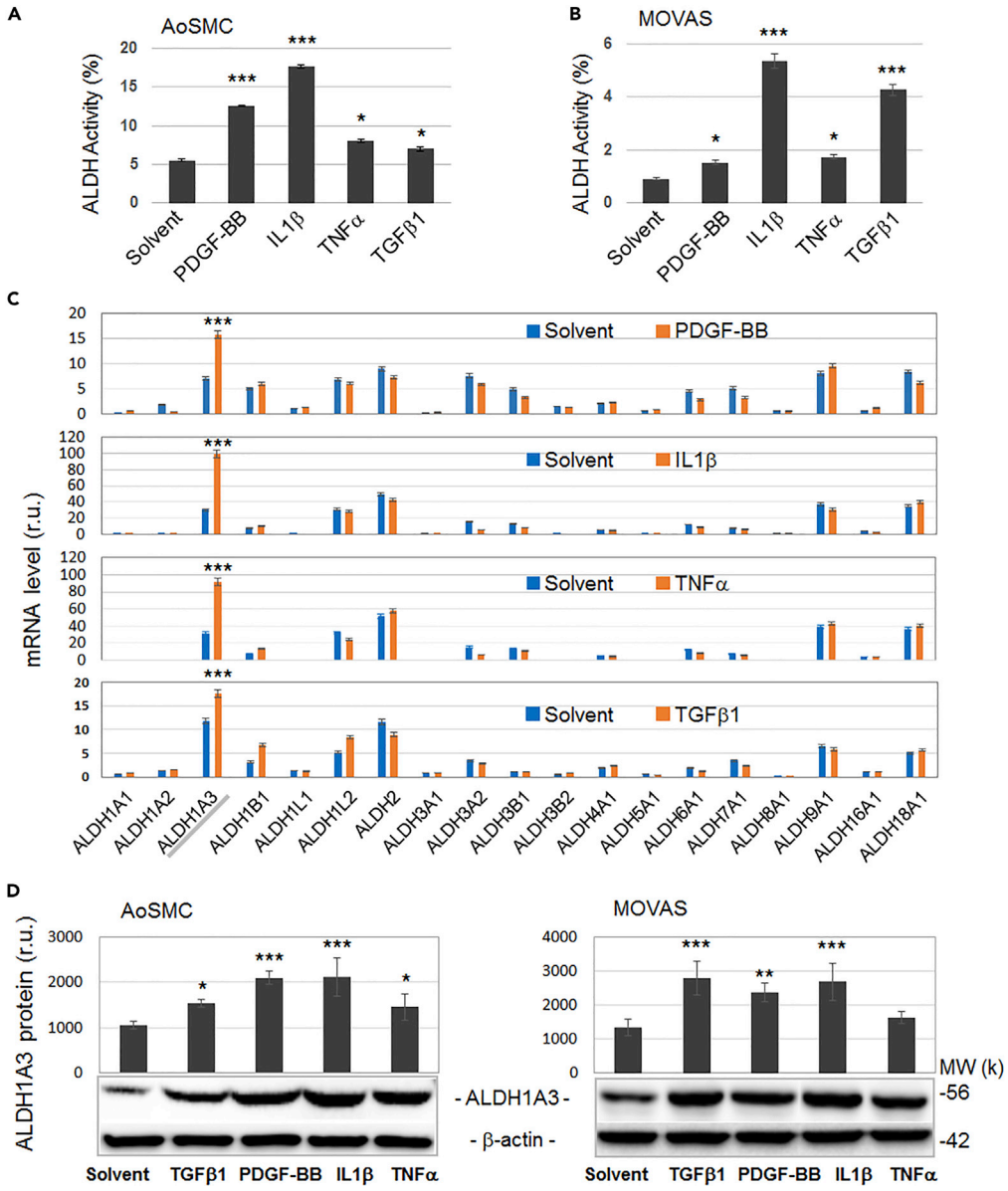

Figure 2. The ALDH1A3 Isoform Predominantly Accounts for Cytokine-Stimulated Increase of VSMC Total ALDH Activity

(A) Increase of ALDH activity in AoSMCs (human) in response to treatment with cytokines.

(B) Increase of ALDH activity in MOVAS (mouse) in response to treatment with cytokines.

(C) Effects of cytokines on mRNA levels of 19 ALDH isoforms.

(D) Effects of cytokines on protein levels of ALDH1A3.

Cultured AoSMCs and MOVAS cells were starved for 24 h and then treated with PDGF-BB (40 ng/mL), IL1β (10 ng/mL), TGFβ1 (20 ng/mL), TNFα (20 ng/mL), or solvent control (4 mM HCl/0.1% BSA) for another 24 h. ALDH activity was determined using fluorescence-activated cell sorting analysis (FACS, see Figure S1) and presented as the percentage of the fluorescently positive cell number versus the total cell number. The mRNA expression of each ALDH isoform was determined using real-time qPCR. For Western blot replicates, samples of equal amount of total protein were loaded, and the exposure time length was kept consistent for the same protein to be detected. The densitometry of ALDH1A3 was normalized to that of beta-actin. Data are expressed as mean ± SE derived from three independent experiments. Student's t test: *$p < 0.05$, **$p < 0.01$, ***$p < 0.001$, each compared with solvent control; r.u., relative unit.

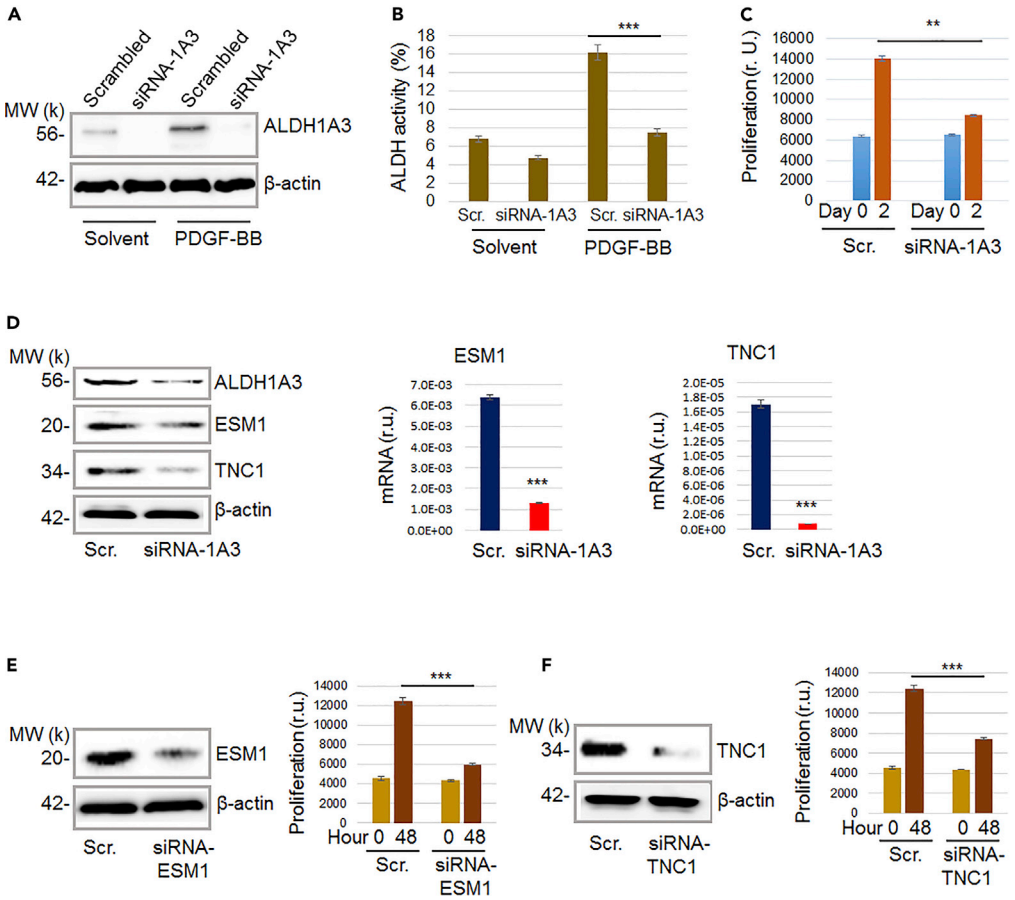

Figure 3. ALDH1A3 Knockdown Reduces ALDH Activity, VSMC Proliferation, and the Expression of ESM1 and TNC1

(A) Western blots indicating efficient ALDH1A3 knockdown.

(B) ALDH1A3 knockdown abolishes the PDGF stimulation of total ALDH activity.

(C) ALDH1A3 knockdown abolishes the PDGF stimulation of AoSMC proliferation (CellTiter-Glo assay).

(D) ALDH1A3 knockdown reduces protein and mRNA levels of ESM1 and TNC1.

(E and F) ESM1 or TNC1 knockdown inhibits AoSMC proliferation.

Human AoSMCs were cultured and treated with solvent control or PDGF-BB as described in Figure 1. For ALDH1A3 knockdown, shRNA was initially used (in A and C) and then siRNA was used throughout (B and D). ALDH activity was determined using fluorescence-activated cell sorting analysis (FACS, Figure S2) and presented as the percentage of fluorescently positive cells versus total cells. mRNA expression of individual ALDH isoform was determined using real-time qPCR. Values were expressed as means ± SE derived from three independent experiments. Student's t test: $^{**}p < 0.01$, $^{***}p < 0.001$, each compared with scrambled control.

Silencing of either ALDH1A3 or ESM1 or TNC1 Mitigates PDGF-Stimulated Activation of AKT/mTOR and/or MEK/ERK Pathways

TNC1 and ESM1 both are matricellular proteins, a special category among ECM proteins that are not major structural elements but play a variety of signaling roles (Balta et al., 2015; Fischer, 2007). We inferred that TNC1 and ESM1 might regulate intracellular signaling that influences VSMC phenotypes. The best-known cytokine-responsive intracellular signaling pathways that strongly influence VSMC phenotypes include the AKT/mTOR/RPS6 pathway and the MAPK pathway. We therefore determined how the activation (phosphorylation) status of those pathways is impacted by silencing ALDH1A3, TNC1, and ESM1 individually. As shown in Figures 4A and 4B, although ALDH1A3 silencing almost completely diminished the levels of phosphor-AKT, phosphor-mTOR, and phospho-RPS6, silencing of ESM1 or TNC1 also substantially reduced phosphorylation of these proteins. Interestingly, silencing either ALDH1A3 or TNC1 diminished protein phosphorylation in the MAPK pathway, including p-MEK, p-ERK, p-p38, and also CyclinD1, a key player in cell division and proliferation, whereas silencing ESM1 did not have an effect on this pathway (Figure 4C).

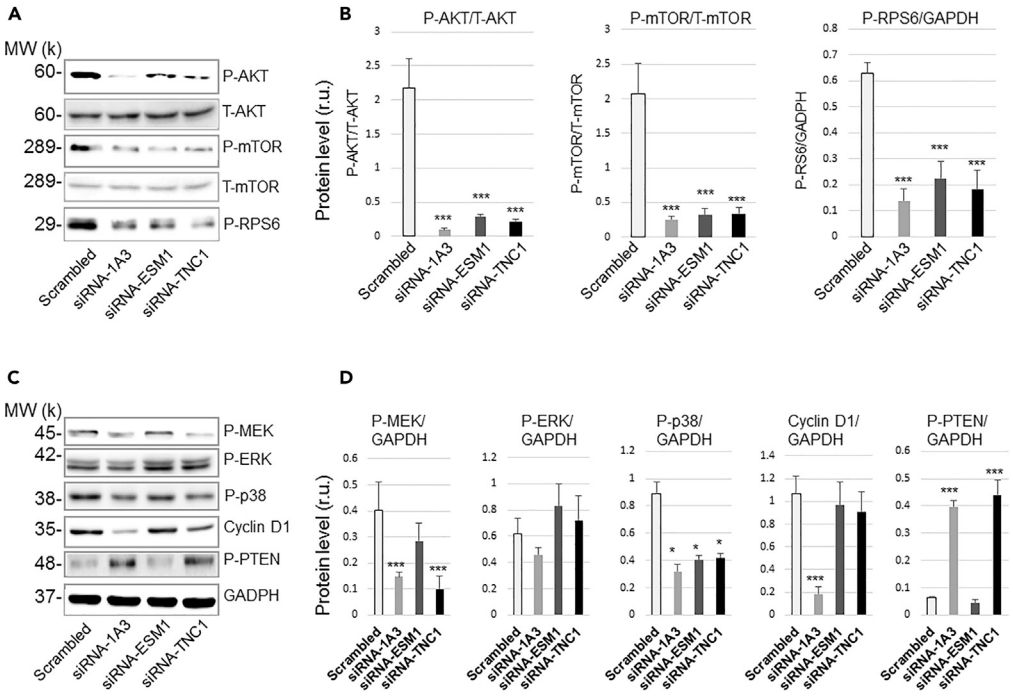

Figure 4. Effects of Gene Silencing of ALDH1A3, ESM1, or TNC1 on the AKT/mTOR and MEK/ERK Signaling Pathways in AoSMCs

(A and B) Western blots of phospho-AKT, phospho-mTOR, and phospho-Ribosomal protein S6 (RPS6) in AoSMCs transfected with a scrambled siRNA (Scr.) or an siRNA to knock down ALDH1A3, ESM1, or TNC1.

(C and D) Western blots of p-MEK, p-p38, and CyclinD1 in AoSMCs transfected with a scrambled siRNA or an siRNA to knock down ALDH1A3, ESM1, or TNC1.

In both (A) and (B), bar graphs show the quantification of protein levels. For western blot replicates, samples of equal amount of total protein were loaded, and the exposure time was kept consistent for the same protein to be detected. Values are expressed as means ± SE derived from three independent experiments. Student's t test: *$p < 0.05$, ***$p < 0.001$, each compared with scrambled control. P, phosphoprotein; T, total protein.

These results indicate that, although ALDH1A3 is responsible for the activation of AKT/mTOR and MAPK pathways, ESM1 and TNC1, both downstream of ALDH1A3, differentially regulate these pathways. Thus, the ALDH1A3-TNC1/ESM1 axis and the downstream regulation of AKT and MAPK pathways may constitute a molecular mechanism that underlies VSMC proliferation induced by elevated ALDH activity.

ALDH Inhibitor DSF Largely Recapitulates the Inhibitory Effect of ALDH1A3 Silencing on PDGF-Stimulated VSMC Proliferation and Intracellular Signaling

Since we elucidated that ALDH1A3 was the isoform that was upregulated and responsible for elevated total ALDH activity and VSMC proliferation after PDGF stimulation (Figure 3), we reasoned that pharmacological ALDH inhibition using DSF should influence VSMC phenotypes and ALDH1A3 downstream signaling similar to that produced by genetic silencing of ALDH1A3. Indeed, pretreatment with DSF dose-dependently inhibited PDGF-stimulated proliferation in all three types of VSMCs (AoSMC, MOVAS, and rat primary SMCs) used for the assays (Figure 5A). DSF also blocked PDGF-stimulated migration of MOVAS and rat SMCs (Figure 5B). We did not observe increased apoptosis in DSF-treated cells (10 μM, MOVAS), indicating low cytotoxicity (Figure 5C). Interestingly, we found that DSF pretreatment preserved the protein level of smooth muscle α-actin (αSMA), which was otherwise reduced by PDGF-BB (Figure 5D). Since reduced αSMA marks a de-differentiated VSMC state, this result further highlights an important role for ALDH1A3 in VSMC phenotypic changes.

Next, we determined the effect of DSF on ALDH1A3-directed intracellular pathways identified previously. DSF preferentially binds ALDH1A3 (IC_{50} = 0.15μM) over other isoforms. As shown in Figure 5D, PDGF-BB stimulation dramatically increased phosphorylation levels of AKT, mTOR, RPS6, MEK, and ERK in AoSMCs,

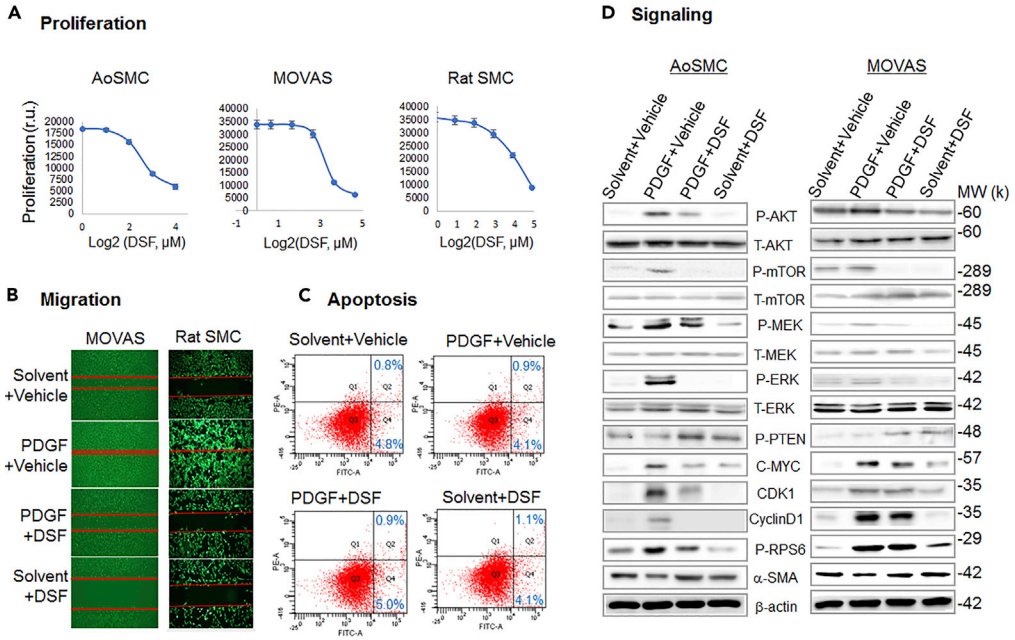

Figure 5. Pan-ALDH Inhibitor DSF Reverses PDGF-stimulated VSMC Phenotypic Changes

AoSMCs, MOVAS cells, or rat SMCs were cultured, starved, and then treated with solvent control or PDGF-BB (as described in Figure 1), with or without pretreatment with 10 μM DSF for 3 h.

(A) DSF inhibits PDGF-stimulated cell proliferation (determined by CellTiter-Glo viability assay). Mean ± SD, n = 3.

(B) DSF inhibits PDGF-stimulated cell migration (scratch assay). Shown are calcein-stained cells 20 h after PDGF-BB stimulation.

(C) DSF does not induce MOVAS cell apoptosis (flow sorting).

(D) DSF inhibits PDGF-stimulated activation of AKT and MEK signaling pathways. Shown are representative blots from at least two similar experiments. P, phosphoprotein; T, total protein.

whereas DSF pretreatment abolished the PDGF-stimulated activation of almost all these proteins. In addition, PDGF-BB upregulated c-Myc, CDK1, and cyclin D1, all well-established factors that drive cell division and proliferation, and pretreatment with DSF attenuated PDGF-stimulated production of these proteins. The experiments using MOVAS largely repeated the results obtained from AoSMCs, although varied degrees of DSF inhibitory effects occurred (Figure 5D).

These results are consistent with the inhibitory effect of DSF on IH (Figure 1) and support ALDH inhibition as an approach to blocking the VSMC phenotypic changes, which are known to play a central role in the development of IH.

Balloon Angioplasty Induces ALDH1A3 Upregulation and DSF Inhibits TNC1 and ESM1 Protein Expression in Injured Rat Carotid Arteries

Based on the *in vitro* results demonstrating PDGF-stimulated ALDH1A3 upregulation and the specific role for ALDH1A3 in mediating VSMC proliferation (Figures 2 and 3), we inferred that ALDH1A3 protein levels could increase in the artery wall when stimulated by injury. We therefore evaluated ALDH1A3 level changes via immunohistochemistry on cross sections of uninjured and balloon-injured rat common carotid arteries that were collected 14 days after balloon angioplasty. Interestingly, the data in Figure 6A showed a 5-fold increase of ALDH1A3 in injured arteries compared with uninjured control. Staining mainly occurred in the neointima lesion and also the medial layer where VSMCs predominately reside, whereas the adventitial layer (mainly fibroblasts) was little stained. We also observed upregulation of the ALDH1A3 protein in the injured artery wall, which provides a logical basis for the mitigation of IH by DSF treatment (Figure 1). Furthermore, our data in Figure 6B indicated that protein levels of TNC1 and ESM1, both increased in injured (mainly in the neointima) versus uninjured arteries, were substantially reduced by treatment with DSF. This result is consistent with the *in vitro* study indicating that ALDH1A3 positively regulates the expression of these two matricellular proteins (Figure 3).

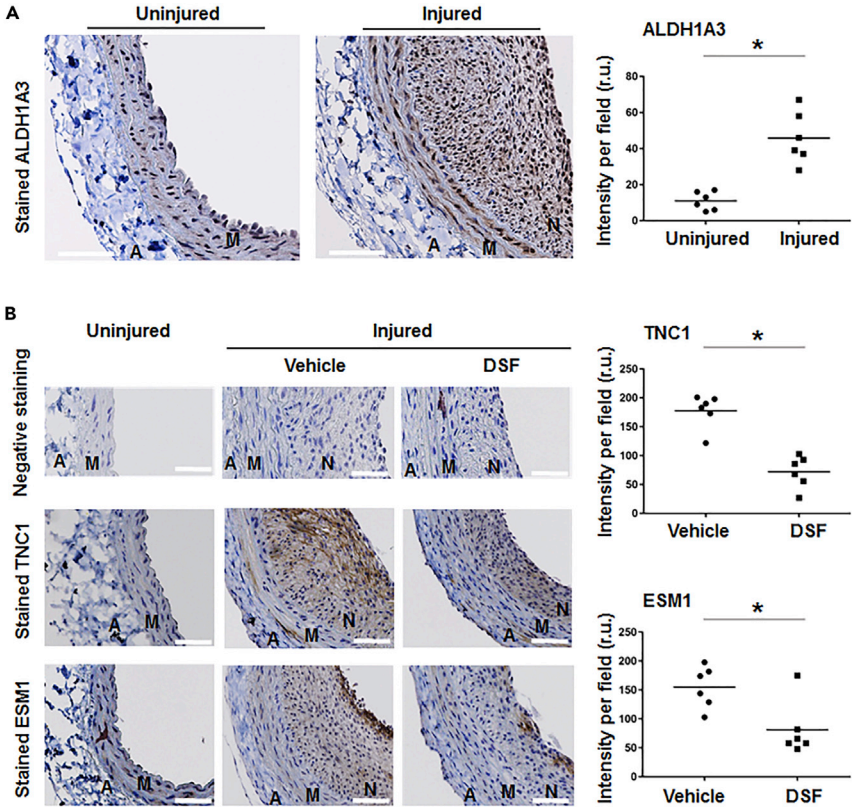

Figure 6. ALDH1A3 Upregulation in Injured Rat Carotid Arteries

Rat carotid artery balloon angioplasty and periadventitial administration of DSF were performed as described in Figure 1. Artery cross sections were immunostained for ALDH1A3 (A) and TNC1 and ESM1 (B). Negative control staining was performed with the same procedures except that primary antibody was omitted. Positive staining was measured as colorimetric intensity per image field and quantified by averaging six to eight sections from each animal, and the averages from all of the six animals in each treatment group were then averaged (see the scatter plots). Student's t test: *$p < 0.05$, ***$p < 0.001$. A, adventitia; M, media; N, neointima. Scale bar: 100 μm.

In summary, the results in this study rationalize an approach to IH suppression via blockade of excessive ALDH activity (or ALDH1A3 protein) following arterial injury.

DISCUSSION

Although IH is widely recognized as a common cause of essentially all occluding vascular diseases, its underlying molecular mechanisms remain inadequately explored. Here, our study reveals a previously unidentified ALDH1A3-directed mechanism that drives the pro-IH phenotypic changes of VSMCs. The major findings are the following: (1) In the entire ALDH family, ALDH1A3 is the isoform that predominantly accounts for the cytokine-stimulated elevation of ALDH activity and proliferation of VSMCs; (2) ALDH1A3 regulates the expression of matricellular proteins (TNC1 and ESM1); (3) Reducing ALDH activity effectively blocks VSMC transition to a pro-IH state. Ultimately, inhibition of ALDH activity can be translated into an IH-mitigating effect in a rat model of restenosis.

Elevated ALDH activity has been linked to cancer cell proliferation and tumorigenesis (Muzio et al., 2012), whereas its contribution to VSMC phenotypic changes and IH remained unclear. Earlier studies showed that ALDH1A1 was mainly responsible for the high ALDH activity in cancer and normal stem cells (Zou et al., 2012). However, this conclusion was challenged by evidence supporting ALDH1A3 as the primary isoform responsible for elevated ALDH activity in some progenitor cell and primitive human mammary cell populations. This discrepancy suggests that differential contributions of ALDH isoforms to total ALDH activity depend on specific cell type/state or disease type and stage. Indeed, via a comprehensive

experimental survey using VSMCs, we found that ALDH1A3 was the isoform that showed predominant mRNA and protein level changes in response to stimulation of a panel of cytokines. Importantly, we obtained compelling evidence that specifically silencing ALDH1A3 alone effectively abolished PDGF-stimulated elevation of total ALDH activity. The involvement of another isoform (ALDH2) in cardiovascular disease has been reported (Mali et al., 2016a). However, our data showed that unlike ALDH1A3, ALDH2 mRNA did not increase under PDGF stimulation, but rather slightly decreased albeit without statistical significance. We thus speculate that ALDH2 may contribute in a different way, e.g., to mitochondrial activities, but not necessarily to PDGF-stimulated VSMC proliferation.

Identifying ALDH1A3 as predominantly responsible for PDGF-stimulated VSMC proliferation enabled us to focus on this isoform and further investigate its regulatory mechanisms. We hence made an unexpected finding of two matricellular proteins (TNC1 and ESM1) as lead candidate effectors downstream of ALDH1A3. ALDH1A3 has been reported to influence various cellular functions, typically progenitor cell proliferation and migration (Puttini et al., 2018). However, to the best of our knowledge, there is no report on ALDH1A3-regulated expression of ECM proteins, including matricellular proteins. This regulation (initially identified via microarray) was verified by inducible ALDH1A3 silencing and Western blotting. Moreover, silencing ALDH1A3, TNC1, or ESM1 inhibited the AKT/mTOR pathway, placing TNC1/ESM1 and ALDH1A3 in the same signaling context. Further consistent evidence was obtained from *in vivo* studies, indicating that, ALDH1A3 expression increased in balloon-injured arteries (versus uninjured control), whereas ALDH inhibition with DSF reduced both TNC1 and ESM1 proteins. Considering possible drug off-target effects, a definitive *in vivo* result requires future experiments using VSMC-specific ALDH1A3 knockout animals.

The finding of TNC1/ESM1 regulation by ALDH1A3 is significant, particularly in view of that matricellular proteins emerge as a unique category of ECM components, whose signaling importance in defining cell differentiation and phenotype has become increasingly appreciated (Puttini et al., 2018). Growing evidence supports a pro-IH role for both TNC1 and ESM1. A few studies showed that increased TNC1 promotes VSMC proliferation and migration (Malabanan et al., 2012; Ishigaki et al., 2011; Sawada et al., 2007). ESM1 was initially identified as an endothelial cell-specific marker mainly produced by ECs. Its function in prompting endothelial inflammation was recently supported by studies of various tissues (Balta et al., 2015). However, ESM1-dependent regulation of VSMC phenotypes was not specifically examined. In this regard, our data have led to another finding in regard to the role of ESM1 in regulating the behaviors of VSMCs; specifically, PDGF-BB stimulated ESM1 expression in VSMCs, and ESM1 silencing inhibited PDGF-stimulated VSMC proliferation.

Taken together, our results and literature evidence unequivocally support a prominent role for both TNC1 and ESM1 in promoting VSMC proliferation, consistent with a scenario where both proteins function in an ALDH1A3-dominated signaling cascade. Indeed, silencing ALDH1A3 maintained inactive AKT/mTOR and MEK/ERK, both pathways with established importance in VSMC proliferation, and silencing TNC1 had a similar effect. Interestingly, silencing ESM1 effectively inhibited the AKT/mTOR pathway but had little effect on MEK/ERK, suggesting a differential ESM1 downstream signaling mechanism as compared with TNC1.

Although intriguing, the result that ALDH1A3 as a metabolic enzyme regulates the gene expression of two matricellular proteins (TNC1 and ESM1) is seemingly counter-intuitive; mechanisms of this regulation remain to be determined. Traces of evidence can be found in the literature. For example, acetyl-Co-A, which could result from ALDH1A3-catalyzed metabolism, is a major source of the acetyl group for histone acetylation (Javaid and Choi, 2017), and H3K27 acetylation opens the chromatin structure thereby promoting transcription. Although plausible, this scenario requires detailed experiments to verify. It is also worth noting that most of the top 20 genes (including TNC1 and ESM1) whose expression is inhibited by DSF pretreatment are matricellular proteins, e.g., PTX3, ASPN, CTGF, PDCD1LG2, CYR61, CLDN11, and HAPLN1 (Figures S3–S5). Further in-depth investigation is warranted to address whether the top "hits" together implicate ALDH1A3-regulated transcription programs for ECM homeostasis.

In summary, our results outline a signaling scheme where increased ALDH1A3 protein/activity upregulates TNC1 and ESM1, which, possibly in an autocrine fashion, activate AKT/mTOR and/or MEK/ERK pathways that drive VSMC proliferation.

Limitations of the Study

One of the limitations is that we used DSF, a pan-ALDH inhibitor, in the microarray experiment. We designed this experiment based on the following rationale: ALDH1A3 but not other isoforms was prominently upregulated under cytokine stimulation; DSF preferentially binds to the ALDH1-class isoforms; a short time (<3 h) needed for pretreatment with a small molecule inhibitor favors observation of direct (versus secondary) effects on gene expression. Future studies will follow to strengthen the microarray results by using ALDH1A3 knockout or knockdown cells. Along this line, although DSF is relatively selective to ALDH1 isoforms over other isoforms (e.g., ALDH2), an ALDH1A3-specific inhibitor (not yet available) is highly desirable as some ALDH isoforms are cytoprotective (Mali et al., 2016a). Considering diverse functions of the ALDH family members, dampening the excessive ALDH activity (elevated owing to injury) rather than eliminating it may provide a viable option for IH mitigation. Another limitation of this study is that, although the *in vivo* DSF inhibition of IH is consistent with the *in vitro* blockage of VSMC proliferation by ALDH1A3 silencing, the *in vivo* process is too complex to be fully explained by *in vitro* results. For example, IH involves not only VSMCs but also ECs and fibroblasts (in the adventitia) in the artery wall. On the other hand, ECs were mostly removed during balloon angioplasty, ALDH1A3 staining was very low in the adventitia layer relative to that in neointima and media layers, and DSF was locally administered around the carotid artery. It is thus reasonable to speculate that the IH-mitigating effect of DSF may have largely occurred via VSMCs in the media and neointima. Nevertheless, more research to delineate ALDH1A3's specific role in IH *in vivo* and to develop isoform-specific ALDH1A3 inhibitors should facilitate translational advancements.

METHODS

All methods can be found in the accompanying Transparent Methods supplemental file.

SUPPLEMENTAL INFORMATION

Supplemental Information can be found online at https://doi.org/10.1016/j.isci.2019.08.044.

ACKNOWLEDGMENTS

This work was supported by NIH grants R01HL-068673 (to K.C.K.), R01HL129785 (to K.C.K. and L.-W.G.), and R01HL133665 (to L.-W.G.).

AUTHOR CONTRIBUTIONS

X.X., L.-W.G., and K.C.K. conceived and designed the study. X.X. performed all the *in vitro* and immunohistochemistry studies. G.U. conducted animal surgery and disease model and morphometric data analysis. L.M. performed sample sectioning. X.X. and L.-W.G. wrote the manuscript. X.X., L.-W.G., M.S., G.U., and K.C.K. revised and critically reviewed the manuscript.

DECLARATION OF INTERESTS

The authors declare no competing interests.

Received: April 11, 2019
Revised: June 9, 2019
Accepted: August 21, 2019
Published: September 27, 2019

REFERENCES

Alexander, M.R., and Owens, G.K. (2012). Epigenetic control of smooth muscle cell differentiation and phenotypic switching in vascular development and disease. Annu. Rev. Physiol. *74*, 13–40.

Balta, S., Mikhailidis, D.P., Demirkol, S., Ozturk, C., Celik, T., and Iyisoy, A. (2015). Endocan: a novel inflammatory indicator in cardiovascular disease? Atherosclerosis *243*, 339–343.

Clowes, M.M., Lynch, C.M., Miller, A.D., Miller, D.G., Osborne, W.R., and Clowes, A.W. (1994). Long-term biological response of injured rat carotid artery seeded with smooth muscle cells expressing retrovirally introduced human genes. J. Clin. Invest. *93*, 644–651.

Cui, J., Li, P., Liu, X., Hu, H., and Wei, W. (2015). Abnormal expression of the Notch and Wnt/beta-catenin signaling pathways in stem-like ALDH(hi)CD44(+) cells correlates highly with Ki-67 expression in breast cancer. Oncol. Lett. *9*, 1600–1606.

Daiber, A., Wenzel, P., Oelze, M., Schuhmacher, S., Jansen, T., and Munzel, T. (2009). Mitochondrial aldehyde dehydrogenase (ALDH-2)–maker of and marker for nitrate tolerance in response to nitroglycerin treatment. Chem. Biol. Interact. *178*, 40–47.

Dey, D., Pan, G., Varma, N.R., and Palaniyandi, S.S. (2015). Sca-1+ cells from fetal heart with high aldehyde dehydrogenase activity exhibit enhanced gene expression for self-renewal, proliferation, and survival. Oxid. Med. Cell Longev. *2015*, 730683.

Fischer, J.W. (2007). Tenascin-C: a key molecule in graft stenosis. Cardiovasc. Res. *74*, 335–336.

Hegab, A.E., Ha, V.L., Bisht, B., Darmawan, D.O., Ooi, A.T., Zhang, K.X., Paul, M.K., Kim, Y.S., Gilbert, J.L., Attiga, Y.S., et al. (2014). Aldehyde dehydrogenase activity enriches for proximal airway basal stem cells and promotes their proliferation. Stem Cells Dev. *23*, 664–675.

Imanaka-Yoshida, K. (2016). Extracellular matrix remodeling in vascular development and disease. In Etiology and Morphogenesis of Congenital Heart Disease: From Gene Function and Cellular Interaction to Morphology, T. Nakanishi, R.R. Markwald, H.S. Baldwin, B.B. Keller, D. Srivastava, and H. Yamagishi, eds. (Springer), pp. 221–226.

Inoue, T., Croce, K., Morooka, T., Sakuma, M., Node, K., and Simon, D.I. (2011). Vascular inflammation and repair: implications for re-endothelialization, restenosis, and stent thrombosis. JACC Cardiovasc. Interv. *4*, 1057–1066.

Ishigaki, T., Imanaka-Yoshida, K., Shimojo, N., Matsushima, S., Taki, W., and Yoshida, T. (2011). Tenascin-C enhances crosstalk signaling of integrin alphavbeta3/PDGFR-beta complex by SRC recruitment promoting PDGF-induced proliferation and migration in smooth muscle cells. J. Cell Physiol. *226*, 2617–2624.

Javaid, N., and Choi, S. (2017). Acetylation- and methylation-related epigenetic proteins in the context of their targets. Genes (Basel) *8*, 1–37.

Malabanan, K.P., Sheahan, A.V., and Khachigian, L.M. (2012). Platelet-derived growth factor-BB mediates cell migration through induction of activating transcription factor 4 and tenascin-C. Am. J. Pathol. *180*, 2590–2597.

Mali, V.R., Deshpande, M., Pan, G., Thandavarayan, R.A., and Palaniyandi, S.S. (2016a). Impaired ALDH2 activity decreases the mitochondrial respiration in H9C2 cardiomyocytes. Cell Signal. *28*, 1–6.

Mali, V.R., Pan, G., Deshpande, M., Thandavarayan, R.A., Xu, J., Yang, X.P., and Palaniyandi, S.S. (2016b). Cardiac mitochondrial respiratory dysfunction and tissue damage in chronic hyperglycemia correlate with reduced aldehyde dehydrogenase-2 activity. PLoS One *11*, e0163158.

Marchitti, S.A., Deitrich, R.A., and Vasiliou, V. (2007). Neurotoxicity and metabolism of the catecholamine-derived 3,4-dihydroxyphenylacetaldehyde and 3,4-dihydroxyphenylglycolaldehyde: the role of aldehyde dehydrogenase. Pharmacol. Rev. *59*, 125–150.

Muzio, G., Maggiora, M., Paiuzzi, E., Oraldi, M., and Canuto, R.A. (2012). Aldehyde dehydrogenases and cell proliferation. Free Radic. Biol. Med. *52*, 735–746.

Puttini, S., Plaisance, I., Barile, L., Cervio, E., Milano, G., Marcato, P., Pedrazzini, T., and Vassalli, G. (2018). ALDH1A3 is the key isoform that contributes to aldehyde dehydrogenase activity and affects in vitro proliferation in cardiac atrial appendage progenitor cells. Front. Cardiovasc. Med. *5*, 90.

Sawada, Y., Onoda, K., Imanaka-Yoshida, K., Maruyama, J., Yamamoto, K., Yoshida, T., and Shimpo, H. (2007). Tenascin-C synthesized in both donor grafts and recipients accelerates artery graft stenosis. Cardiovasc. Res. *74*, 366–376.

Szabo, A.Z., Fong, S., Yue, L., Zhang, K., Strachan, L.R., Scalapino, K., Mancianti, M.L., and Ghadially, R. (2013). The CD44+ ALDH+ population of human keratinocytes is enriched for epidermal stem cells with long-term repopulating ability. Stem Cells *31*, 786–799.

Tratwal, J., Mathiasen, A.B., Juhl, M., Brorsen, S.K., Kastrup, J., and Ekblond, A. (2015). Influence of vascular endothelial growth factor stimulation and serum deprivation on gene activation patterns of human adipose tissue-derived stromal cells. Stem Cell Res. Ther. *6*, 62.

Triscott, J., Rose Pambid, M., and Dunn, S.E. (2015). Concise review: bullseye: targeting cancer stem cells to improve the treatment of gliomas by repurposing disulfiram. Stem Cells *33*, 1042–1046.

Wang, B., Zhang, M., Takayama, T., Shi, X., Roenneburg, D.A., Craig Kent, K., and Guo, L.W. (2015). BET bromodomain blockade mitigates intimal hyperplasia in rat carotid arteries. EBioMedicine *2*, 1650–1661.

Woods, T.C. (2013). Dysregulation of the mammalian target of rapamycin and p27Kip1 promotes intimal hyperplasia in diabetes mellitus. Pharmaceuticals (Basel) *6*, 716–727.

Young, K., Tweedie, E., Conley, B., Ames, J., Fitzsimons, M., Brooks, P., Liaw, L., and Vary, C.P. (2015). BMP9 crosstalk with the hippo pathway regulates endothelial cell matricellular and chemokine responses. PLoS One *10*, e0122892.

Zhang, L., Wang, H., Xiao, M., Kudinha, T., Mao, L.L., Zhao, H.R., Kong, F., and Xu, Y.C. (2014). The widely used ATB FUNGUS 3 automated readings in China and its misleading high MICs of Candida spp. to azoles: challenges for developing countries' clinical microbiology labs. PLoS One *9*, e114004.

Zou, B., Sun, S., Qi, X., and Ji, P. (2012). Aldehyde dehydrogenase activity is a cancer stem cell marker of tongue squamous cell carcinoma. Mol. Med. Rep. *5*, 1116–1120.

ISCI, Volume *19*

Supplemental Information

ALDH1A3 Regulations of Matricellular Proteins Promote Vascular Smooth Muscle Cell Proliferation

Xiujie Xie, Go Urabe, Lynn Marcho, Matthew Stratton, Lian-Wang Guo, and Craig K. Kent

Supplemental Figures

Figure S1A

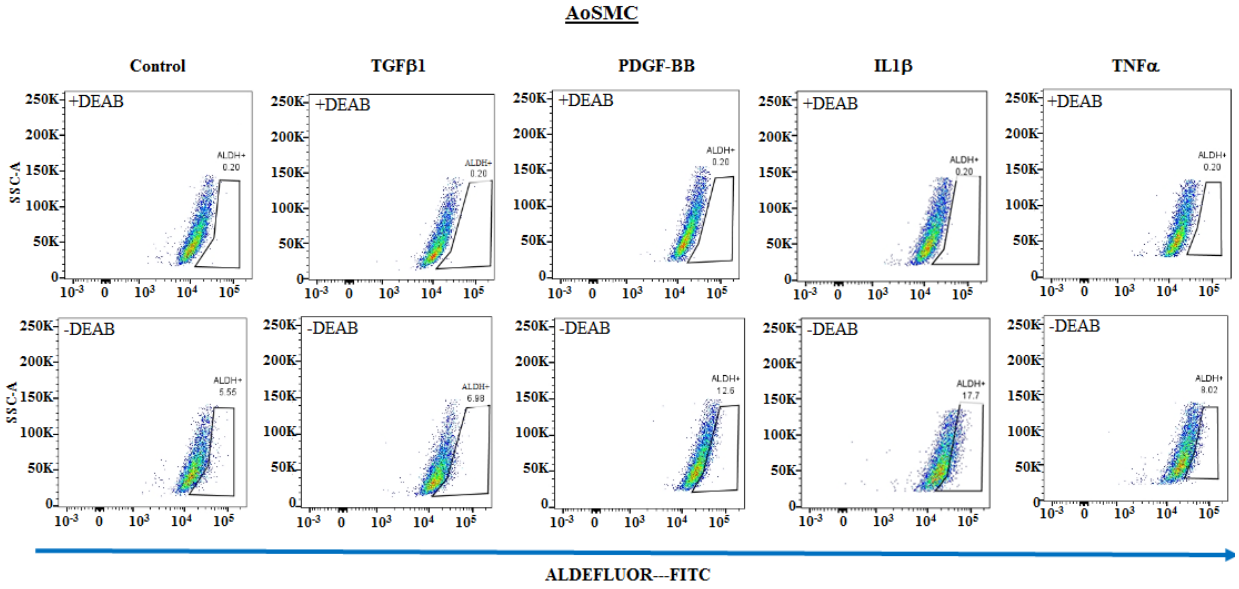

Figure S1B

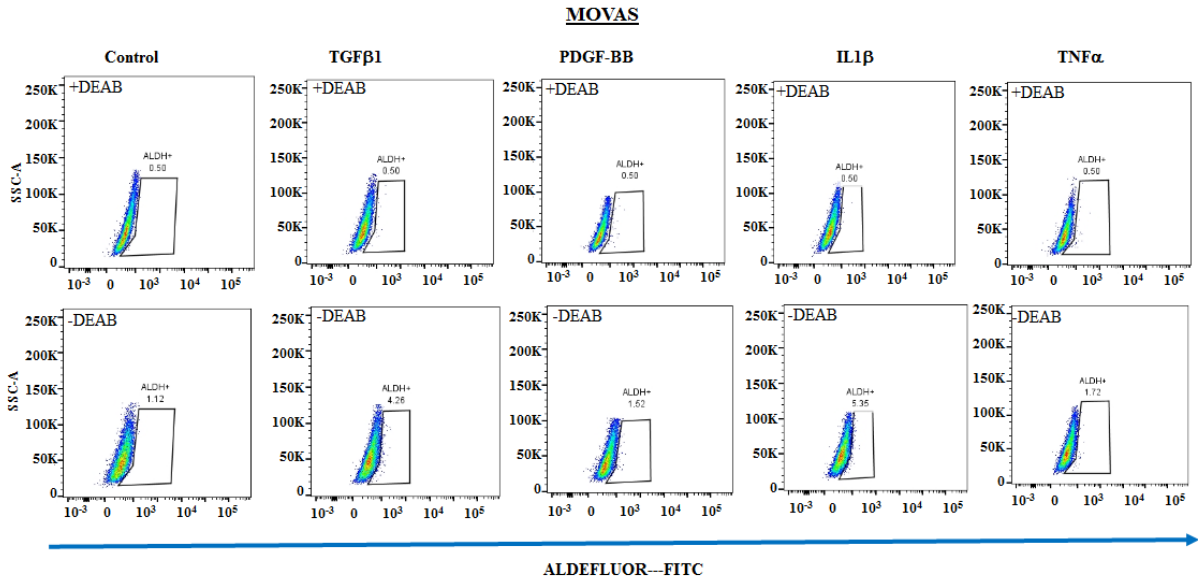

Figure S1. Related to Figure 2. *Fluorescence-activated cell sorting (FACS) analysis of total ALDH activity of VSMCs stimulated by cytokines*

Cultured AoSMCs (A) and MOVAS (B) cells were starved and treated with PDGF-BB (40 ng/ml), IL1β (10 ng/ml), TGFβ1 (20 ng/ml), TNFα (20 ng/ml), or solvent control (4mM HCl/0.1% BSA), as described in Figure 1. ALDH activity was measured (using FACS) as % fluorescently positive cells versus the total cell number.

Figure S2

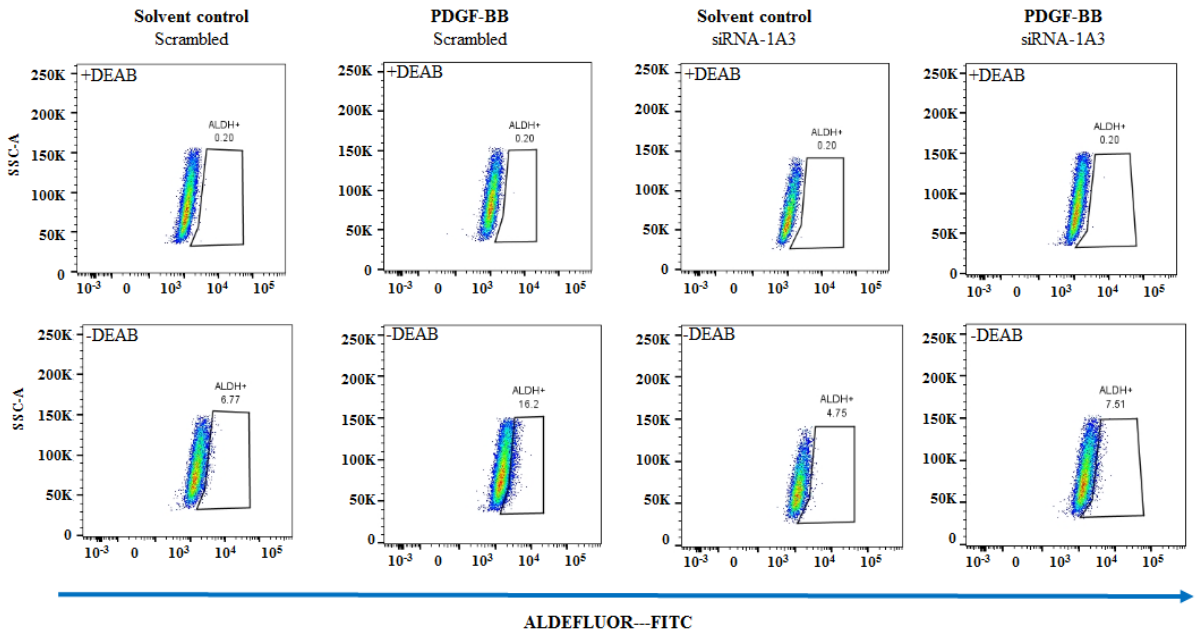

Figure S2. Related to Figure 3. ***FACS analysis of the effect of ALDH1A3 silencing on total ALDH activity***

Experiments were performed as described in Figure 3B. ALDH activity was measured (using FACS) as % fluorescently positive cells versus the total cell number.

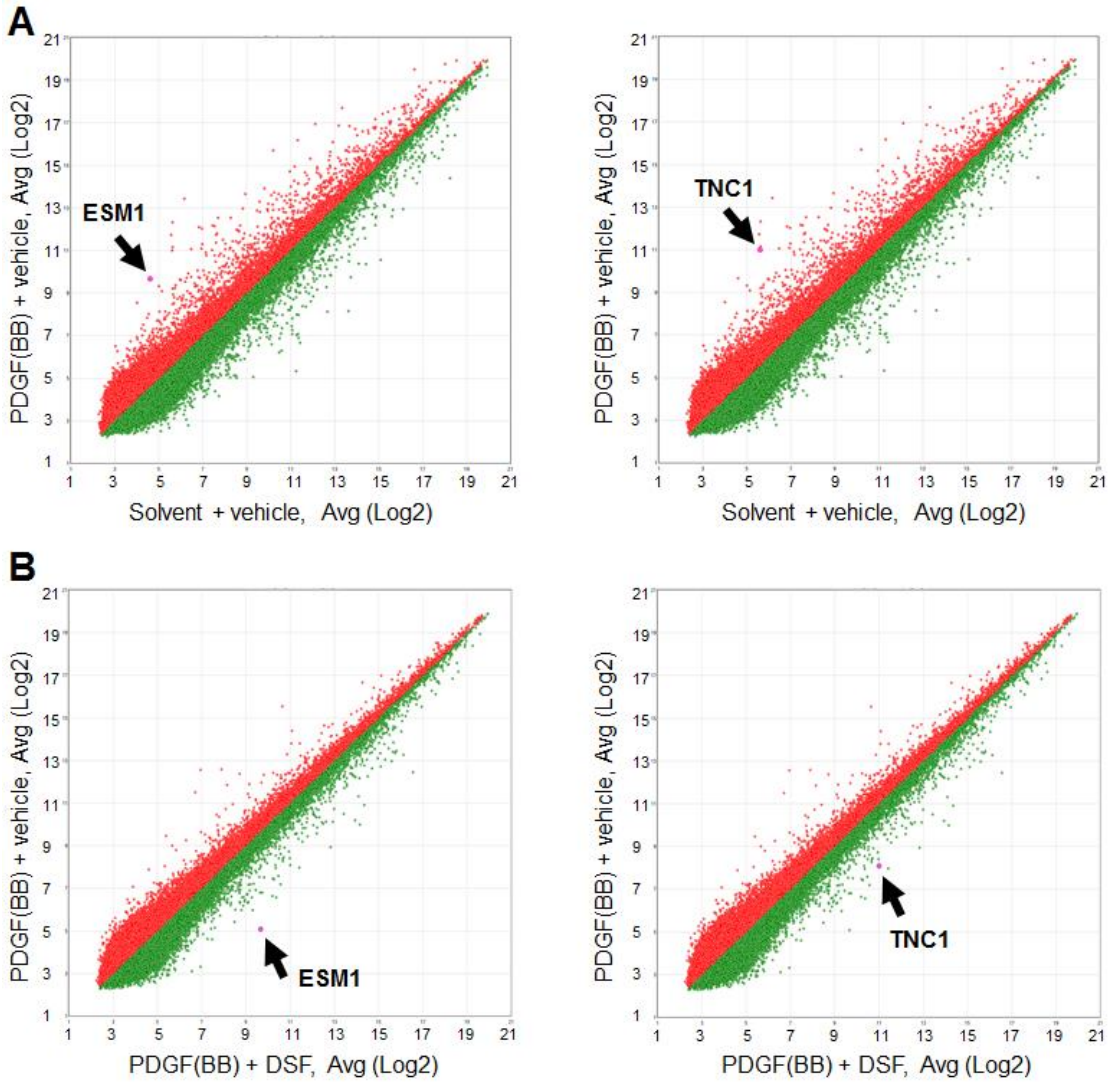

Figure S3. Related to Figure 3. ***Gene array for identification of genes whose expression changes after treatment with PDGF-BB and/or DSF pretreatment***
AoSMCs were cultured, starved, and then treated with solvent control or PDGF-BB for 20 hours with or without 3h-pretreatment with 10 μM DSF, as described for Figure 5. The cells were then used for Affymetrix microarrays (Human Transcriptome Array 2.0) at the Ohio State University Comprehensive Cancer Center – James Hospital Shared Resources and Core Facilities. The data were obtained from duplicate samples for each condition, and analyzed using Transcriptome Analysis Console. Shown are all of the genes identified.

A. ESM1 or TNC1 gene expression was upregulated by PDGF stimulation (versus solvent control).
B. ESM1 or TNC1 gene expression was down-regulated by pretreatment with DSF (versus vehicle control) in the presence of PDGF stimulation.

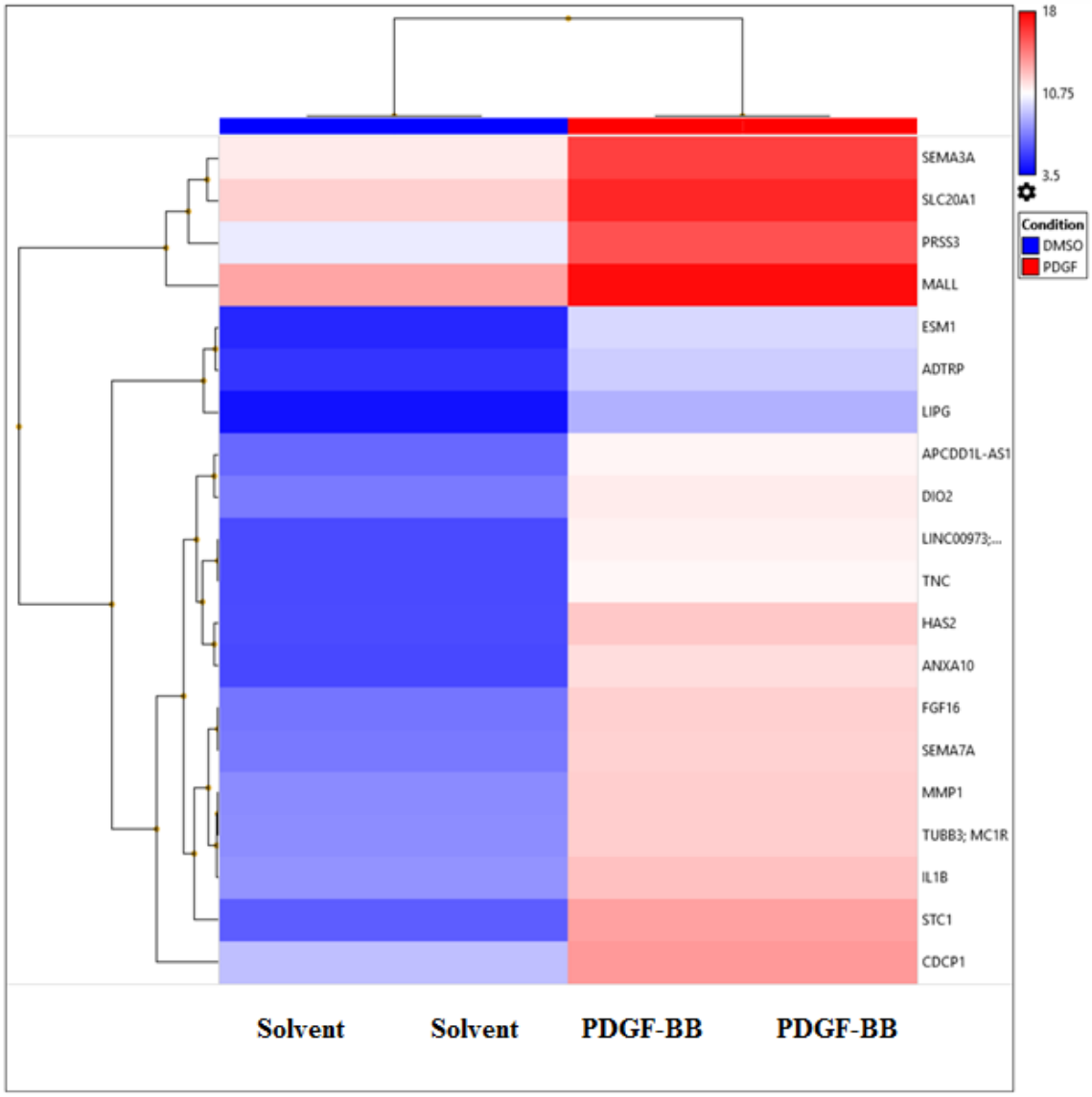

Figure S4. Related to Figure 3. ***Gene array for identification of top-20 genes upregulated by PDGF-BB***

AoSMC culture, Affymetrix microarrays, and data analysis were performed as described for Figure S3. Shown are top 20 genes upregulated after treatment with PDGF-BB.

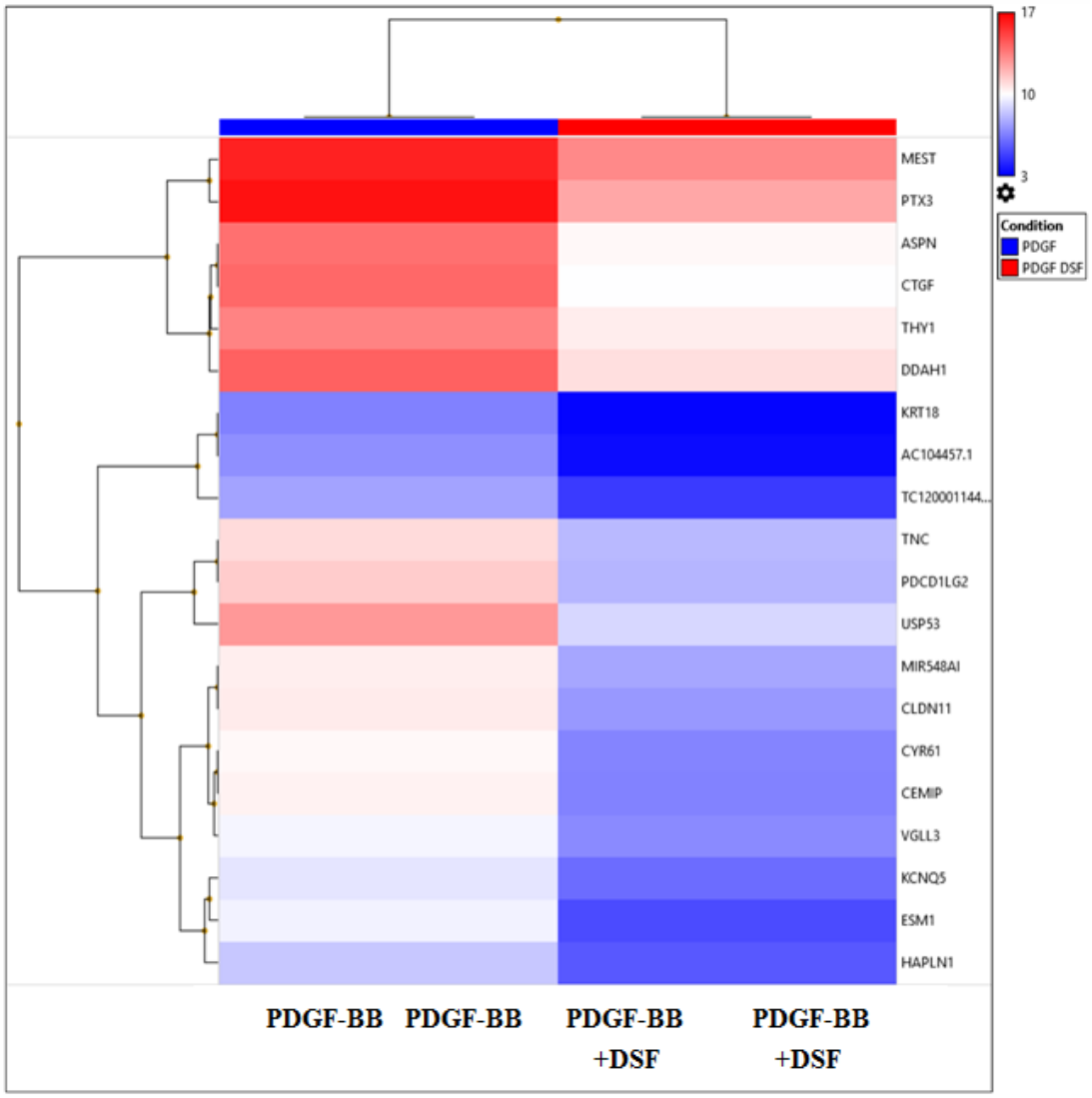

Figure S5. Related to Figure 3. ***Gene array for identification of top-20 genes down-regulated by ALDH activity***

AoSMC culture, Affymetrix microarrays, and data analysis were performed as described for Figure S3. Shown are the top 20 genes that were down-regulated by DSF in the presence of PDGF-BB stimulation

Note only the ESM1 and TNC1 genes are on both Figure S4 and S5 top-20 lists.

Supplemental Tables

Table S1. Related to Figure 3. ***Primers used for qRT-PCR***

Gene	Forward	Reverse
ESM1	5'-AAGGC TGCTGATGTAGTTC-3'	5'-GCTATTTATGGAAGT GTATGTGTTT- 3'
TNC1	5'-CCATCAGTACCACGGCTACC-3'	5' – CCCTTCATCAGCAGTCCAGG- 3'
GADPH	5'-CATGTTCGTCATGGGTGTGAACCA- 3'	5'-ATGGCATGGACTGTGGTCATGAGT- 3'

Table S2. Related to Figures 4,5,6. ***Antibodies for Western blotting and IHC***

antibody	**company**	**Cat#**	**Dilution**
Western blotting			
ALDH1A3	Abcam	ab129815	1:1000
beta-actin	Abcam	ab6276	1:5000
phospho-AKT	Cell Signaling Technology	4060	1:2000
Phospho-p44/42 MAPK (Erk1/2) (Thr202/Tyr204)	Cell Signaling Technology	4370	1:2000
Phospho-MEK1 (Thr286)	Cell Signaling Technology	9127	1:1000
Phospho-mTOR (Ser2448)	Cell Signaling Technology	5536	1:1000
Phospho-S6 Ribosomal Protein (Ser235/236)	Cell Signaling Technology	4858	1:2000
Phospho-PTEN (Ser380/Thr382/383)	Cell Signaling Technology	9554	1:1000
AKT (pan)	Cell Signaling Technology	4691	1:1000
44/42 MAPK (Erk1/2)	Cell Signaling Technology	4695	1:1000
MEK1/2 (L38C12)	Cell Signaling Technology	4694	1:1000

mTOR (7C10)	Cell Signaling Technology	2983	1:1000
c-Myc (D84C12)	Cell Signaling Technology	5605	1:1000
Cyclin D1	Abcam	ab134175	1:20000
CDK1	Abclonal	A0220	1:500
ESM1	Santa Cruz	sc-515304	1:200
TNC1	Abcam	ab108930	1:2000
IHC			
ALDH1A3	Abcam	ab129815	1:200
ESM1	Abcam	ab224591	1:100
TNC1	Abcam	ab108930	1:200

Table S3. Related to Figure 3. *shRNA (ALDH1A3) sequences*

1	5’ AAAAGGTCAAGTTCACCAAGATATTGGATCCAATATCTTGGTGAACTTGACC 3’
2	5’ AAAAGCAGAGAACTAGGTGAATATTGGATCCAATATTCACCTAGTTCTCTGC 3’
3	5’AAAAGCAGGTCTACTCTGAGTTTGTTTGGATCCAAACAAACTCAGAGTAG ACCTGC3’

Transparent Methods

Materials

Human Aortic smooth muscle cells (AoSMCs, CC-2571), smooth muscle cell basal medium (SmBM, CC-3181), and SmBM plus SingleQuots of supplements (CC-3182) were purchased from Lonza. The mouse aortic smooth muscle cell line MOVAS was purchased from ATCC (CRL-2797). Dulbecco's modified Eagle's medium (DMEM, 11965118) was from Invitrogen. Lenti-X™ 293T cell line was purchased from Clontech (632180). Recombinant Human TGF-beta 1 (240-B), TNF-alpha (210-TA), IL-1 beta (201-LB), and PDGF-BB (520-BB), were purchased from R&D Systems. ALDH inhibitor, DSF (cat#1224008) was purchased from Sigma-Aldrich (St. Louis, MO). Cell Titer-Glo 2.0 Assay kit was purchased from Promega (G9242). For ImmPRESS™ HRP Anti-Rabbit IgG (Peroxidase) Polymer Detection Kit (MP-7451-15) and ImmPACT DAB Peroxidase (HRP) Substrate (SK-4105) were purchased from Vector Laboratories.

Vascular smooth muscle cell culture and cytokine treatment

AoSMCs were cultured in SmBM with supplements. Cells were passaged every 2-3 days at a ratio of 1:3. Cells used in this study were below passage 8. MOVAS cells were cultured in DMEM supplemented with 4.5g glucose, 10% Fetal Bovine Serum (FBS), and Penicillin-Streptomycin (Thermo Fisher Scientific, 15140122). Rat smooth muscle cells (SMCs) were isolated from the thoracoabdominal aorta of adult male Sprague-Dawley rats as described by Clowers et al (Clowes et al., 1994). Rat SMCs were cultured in DMEM supplemented with 1g glucose, 10% FBS, and Penicillin-Streptomycin. Rat SMCs below Passage 5 were used in this study. All cultured cells were maintained in a humidified incubator with 5% CO_2 at 37 °C. All cytokine treatments were 20 hours after 24 hours starvation (SmBM for AoSMC, DMEM with 0.5% FBS for MOVAS, and DMEM with 0.2% FBS for rat SMCs).

ALDH activity assay

The total ALDH activity of VSMCs was determined using the ALDEFLUOR kit (01700) according to the manufacturer's protocol from Stem Cell Technologies, British Columbia, Canada. Cells were suspended in ALDEFLUOR assay buffer containing ALDH substrate (bidipy-aminoacetaldehyde, 1 mM per 1 x 10^6 cells) and incubated for 45 min at 37 ℃. For each experiment, a sample of cells was incubated with 50 mM of diethylaminobenzaldehyde (DEAB), an ALDH inhibitor, to serve as the negative control. Cells were spun down at 300 $\times g$ for 5 min at 4 ℃ and re-suspended in 0.5 ml ALDEFLUOR assay buffer for analysis. Fluorescence-activated cell sorting analyses were performed using BD FACS Calibur at the Ohio State University Comprehensive Cancer Center Analytical Cytometry Core.

Quantitative real-time PCR (qRT-PCR)

Total RNA was extracted from cell lysates using the TRIzol reagent or TaqMan PreAmp Cells-to-CT kit (both from ThermoFisher Scientific, Waltham, MA). The mRNA expression of ALDH isoforms was determined using the Applied Biosystems 7900HT Fast Real-Time PCR System

with validated TaqMan primers (ThermoFisher Scientific). The mRNA levels of ALDH isoforms were normalized to glyceraldehyde 3-phosphate dehydrogenase (GADPH) using the ΔΔCt method. qRT-PCR primers are listed in Table S1.

Western blotting

Cells were lysed in RIPA buffer (50 mM Tris, 150 mM NaCl, 1% Nonidet P-40 and 0.1% sodium dodecyl sulfate) containing Halt™ Protease and Phosphatase Inhibitor Cocktail Cocktail (Thermo Fisher Scientific, 78440). Protein concentration was determined using a Pierce BCA Protein Assay kit (Thermo Fisher Scientific, 23227). Whole-cell lysates were mixed with Laemmli loading buffer, boiled, separated by 12% SDS–PAGE and transferred to a PVDF membrane. Subsequently, immunoblot analyses were performed using specific antibodies (source companies, catalog numbers and dilution ratios listed in Table S2). The signal was developed using the Western Blotting Kit (Pierce, 35050).

Silencing of ALDH1A3, TNC1 and ESM1

For ALDH1A3 knockdown, an shRNA expression system was intitially used in the proliferation experiments. Three targeting sequences (Table S3) were designed, synthesized, and cloned into the inducible tetracycline-on pLV-RNAi (BioSettia, San Diego, CA) vector. Cells were transduced with pLV-RNAi/shRNA-ALDH1A3 and polyclonal cell populations were collected. Preliminary studies demonstrated that sequence 1 was the most efficient to knockdown ALDH1A3, which was used for proliferation data collection. Knockdown was induced by doxycycline at 1000 ng/ml. As indicated in figure legends, siRNAs were used through out the remaining experiments. Silencer Select siRNA products were purchased from Thermo Fisher Scientific: siRNA-ALDH1A3 (ID:s32, cat# 4427038), siRNA-ESM1 (ID:s21850, CAT#4427037), and siRNA-TNC1 (ID: s224742, cat#4427037).

Cell Titer-Glo cell viability assay

The assay was performed as we previously reported (Wang et al., 2015). Briefly, AoSMC, MOVAS, or Rat smooth muscle cells were starved for 24 hours, and then pretreated with DSF for 3 hours before PDGF-BB (50 ng/ml) treatment. At 48 hours after treatment of PDGF-BB, cells were washed with PBS once and then 50 μl of PBS and 50 μl of CellTiter-Glo reagent were added into each well. The 96-well plate was then analyzed using the Flexstation 3 plate reader. To keep the experimental condition consistent, we typically seeded cells at a density of 2000 cells per well and performed the CellTiter-Glo assay at a cell confluency no more than 70-80%. To measure cell proliferation in gene knockdown experiments, cell number counting was performed using a cellometer.

Scratch assay for cell migration

MOVAS or rat SMCs were grown in 6-well culture plate to 90% confluence. After 24 hours starvation, cells were pretreated with DSF for 3 hours. A scratch wound was then made with a sterile pipette tip across the cell monolayer followed by adding 50 ng/mL of PDGF-BB. The area that was reoccupied by migrating cells was determined after 20 hours.

Cell apoptosis assay

After 24 hours of starvation, MOVAS cells were treated for 24 hours with solvent control or PDGF-BB, with or without a 3-hour pretreatment with 10 μM DSF. Cells were harvested and washed with cold PBS, and resuspended to 10^6 cells/mL in 1× annexin-binding buffer with 5 μL of FITC annexin V and 1 μL of the 100 μg/mL PI working solution added to each 100 μL of cell suspension. After 15 min incubation at room temperature, 400 μL of annexin-binding buffer were added to each 100 μL of cell suspension. Apoptotic cells were analyzed using BD FACS Calibur (BD Biosciences Corporation, Franklin Lakes, NJ, USA) at the Ohio State University Comprehensive Cancer Center Analytical Cytometry Core.

Animals

Male Sprague-Dawley rats were purchased from Charles River Laboratories (Wilmington, MA). All animal experiments were carried out in accordance with the recommendations in the Guide for the Care and Use of Laboratory Animals of the National Institutes of Health. The protocol was approved by the Institutional Animal Care and Use Committee (IACUC) of The Ohio State University. Isoflurane general anesthesia was used during surgery (through inhaling, oxygen flow rate 2 L/minute) and buprenorphine was subcutaneously injected (0.03 mg/kg, 0.01 mg/rat) after the surgery. Animals were euthanized in a chamber gradually filled with CO_2.

Rat carotid artery balloon injury model

Rat carotid artery balloon injury was performed as we previously described (Wang et al., 2015) with minor modifications. Briefly, after induction of general anesthesia with isoflurane, a 2-French balloon catheter (Edwards Lifesciences Corp., Irvine, CA) was inserted through the left external carotid artery into the common carotid artery of male Sprague-Dawley rats (300~350 g), insufflated with 1.5 atm of pressure, and then retracted to the distal bifurcation. This action was repeated for four times, and the catheter was rotated while being retracted at the 4^{th} time. The external carotid artery was then ligated, and blood flow was resumed. Immediately following the surgery, vehicle control (DMSO) or DSF (9 mg/rat) carried in a thermosensitive hydrogel (AK12, Akina Inc., West Lafayette, IN) was applied to the periadventitial space surrounding the injured common carotid artery. The neck incision was then closed and sanitized, and the animal was left on the warm pad to recover. Isoflurane general anesthesia was applied during surgery (through inhaling, oxygen flow rate 2 L/minute) and buprenorphine was subcutaneously injected (0.03 mg/kg, 0.02 mg/rat) after the surgery. The rats were euthanized 14 days after surgery and common carotid arteries were collected after perfusion fixation with 4% paraformaldehyde (PFA). The collected arteries were further fixed in 4% PFA overnight and then processed for sectioning and morphometric analysis.

Morphometric analysis of intimal hyperplasia (IH)

Paraffin-embedded arteries were cut into 5-μm sections for hematoxylin-eosin (H&E) staining. The intima area and media area were measured on the sections and calculated using ImageJ. Intima area was calculated as internal elastic lamina (IEL) area minus lumen area; Media area

was calculated as external elastic lamina (EEL) area minus IEL area. Measurements were performed by a student blinded to the experimental conditions. IH was quantified as a ratio of intima area vs media area (I/M ratio). The data was generated by averaging 6 to 8 sections from each animal. The averages from all of the 6 animals in each treatment group were then averaged.

Immunohistochemistry

Paraffin-embedded arteries were cut into 5-μm sections for immunostaining analysis. Artery slides were deparaffinized and rehydrated through xylenes and graded alcohol series. Antigen retrieval was done using citrate buffer for 2 hours at 80ºC in a high pressure cocker. Endogenous peroxidase was blocked by incubation with 3% H_2O_2 for 10 min. ImmPRESS™ HRP Anti-Rabbit IgG (Peroxidase) Polymer Detection Kit (Vector Laboratories, MP-7451-15) was used to perform immunostaining of ALDH1A3, ESM1, and TNC1. Antibodies: ALDH1A3, Abcam, ab129815; ESM1, Abcam, Ab224591; TNC1, Abcam, Ab108930. The staining intensity was visualized using ImmPACT DAB Peroxidase (HRP) Substrate. Six different fields were then imaged from each section at ×400.

Statistical analysis

Values were expressed as means ± SE derived from three independent experiments. Statistical analyses were performed with Prism 5.0 (GraphPad Software). Differences between two groups were analyzed by two-tailed Student's *t*-test. *P* values <0.05 were considered as statistically significant.

References

CLOWES, M. M., LYNCH, C. M., MILLER, A. D., MILLER, D. G., OSBORNE, W. R. & CLOWES, A. W. 1994. Long-term biological response of injured rat carotid artery seeded with smooth muscle cells expressing retrovirally introduced human genes. *J Clin Invest,* 93**,** 644-51.

WANG, B., ZHANG, M., TAKAYAMA, T., SHI, X., ROENNEBURG, D. A., CRAIG KENT, K. & GUO, L. W. 2015. BET Bromodomain Blockade Mitigates Intimal Hyperplasia in Rat Carotid Arteries. *EBioMedicine,* 2**,** 1650-1661.